

A novel image enhancement approach for Phalanx and Epiphyseal/metaphyseal segmentation based on hand radiographs

Chih-Yen Chen, Tai-Shan Liao

Electronics Shop

Instrument Technology Research Center, National Applied
Research Laboratories
Hsinchu, Taiwan
cychen@itrc.narl.org.tw

Chi-Wen Hsieh

Department of Electrical Engineering
National Chiayi University
Chiayi, Taiwan

Tzu-Chiang Liu

Department of radiology
Taipei Veterans General Hospital
Taipei, Taiwan

Hung-Chun Chien

Department of Electronic Engineering
Jinwen University of Science and Technology
New Taipei City, Taiwan

Abstract—Precise and effective bony segmentation from soft tissues on hand radiograph is very critical in the bone age assessment, especially for separating phalanx and epiphyseal/metaphyseal region of interests (EMROIs) from the background and soft tissue. Our aim is to locate and segment the EMROIs based on children's hand radiographs, in which the images are with nonuniform background. Furthermore, a great destructive noise may suppress the segmentation process. The proposed approach combines a series of image preprocessing procedures to crop the left-hand radiograph and EMROIs. The experiments were conducted on different parts of knuckles, such as distal, middle, and proximal. Finally, the segmentation results demonstrate that the proposed schemes can segment the EMROIs automatically and effectively for the extraction of characteristics of bone age assessment.

Keywords- Bone age, Segmentation, Epiphyseal, Metaphyseal, Neutrosophic set, K-means clustering

I. INTRODUCTION

Bone age (BA) is significant for diagnosing the growth potential of children. Clinically, pediatricians make a decision for a child with growth disorders, growth hormone deficiency, and the efficacy of growth therapy by determining if the discrepancy between the BA and the chronological age (CA) is consistent. Thus, the bone age assessment (BAA) is widely applied by evaluating the ossifications of carpal, phalanges, ulna and radius, and the epiphysis/metaphysis.

Greulich and Pyle (GP) atlas [1] and Tanner-Whitehouse III (TW) method [2] are two preferred methods which can help the pediatricians and radiologists evaluate children's BA. The former is to test the consistency of the left-hand radiograph and the corresponding chronological age (CA) by a visual comparison with standard atlas of hand radiograph. Then, the best matching standard can be selected as the appropriate

pattern. Such an approach allows most pediatricians to determine BA easily, but human subjectivity and qualitative analysis cause the operation be lack of repeatability and reliability [3,4]. Comparing to TW method, the usage is to assess the BA by assessing the detailed shape analyses of several bones of interest and conducting to corresponding scores. Subsequently, to sum up all the TW scores, the most approaching bone stages can be determined. Accordingly, the TW method serves a more objective examination than the GP method, but the drawbacks of complexity and time-consuming cause TW method relatively rare use in clinical practice [3].

An increasing attention has been paid to the development of automatic computerized analyses of BA by using a series of image processing techniques. The advantages of BAA are including reproducibility and reliability; therefore, many reports focusing on the precise computer-based BAA have been made for improving the performance [4,5]. In that work, image segmentation can be seen as the most difficult tasks in the BAA. Therefore, another grayscale-histogram morphology algorithm, or a gamma parameter enhancement algorithm for the segmentation of phalanx (PROIs) and epiphyseal/metaphyseal region of interests (EMROIs) was suggested to achieve the goal with the greatest possible precision [6,7].

As for the gray-level image segmentation, the extent of similar brightness and the gray levels of neighboring pixels at the boundaries of the sub-blocks change, can have certain influence on the detection of isolated points, lines and edges. In generally, the approaches based on homogeneity and intensity can be attributed to thresholding, edge detection, clustering and region growing [8]. Recently, a new novelty of neutrosophic set (NS) concept, proposed by Florentin Smarandache as a new branch of philosophy dealing with the origin, nature and scope of neutralities, as well as their

applications in the different ideational spectra [9]. As neutrosophy theory mentioned, each event or entity has a certain degree of truth, a falsity degree and an indeterminacy degree that can be defined as independent from each other.

In our study, the EMROIs are extracted by using a series of image preprocessing procedures. Next, the initial image enhancement based on gray level distribution was adopted to make the phalanx contour region clear. Following, the k-means clustering algorithm was applied to separate epiphysis and metaphysis from the soft tissue and background.

II. EXPERIMENT METHODS

Initially, the lower resolution version of hand radiograph reduce the computation time, and therefore the images was resized to a fixed scale of 0.25 for improve the computation time. Next, the hand radiographs contain some artifacts of labels and noises, which interfere with the segmentation framework. Therefore, to find a background image can be helpful to suppress the nonuniformity for improving the hand-to-background ratio [10]. Subsequently, a profile of top-bottom scan was executed to find out the edge of left-hand region. Finally, the left-hand can be successfully cropped. The schematic representation of pre-processing stage is demonstrated in Fig. 1.

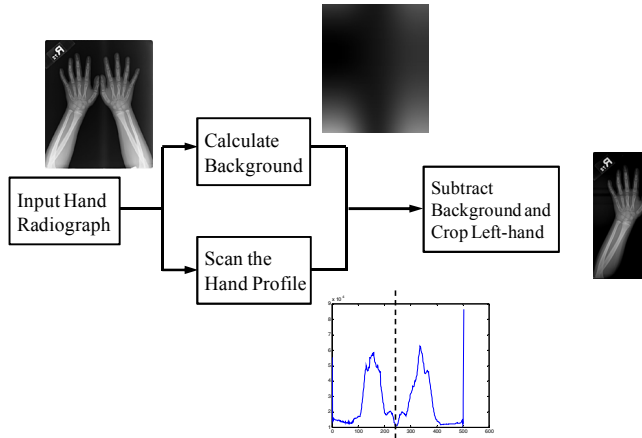


Figure 1. Schematic diagram of cropped left-hand radiograph.

Generally, the cropping left-hand radiograph is not a purified image for extracting the middle finger. To locate and segment the middle finger precisely, several further processes are suggested. The heuristic procedures shown in Fig. 2 are explained below.

- Acquire the cropped left hand image.
- Binary the left-hand radiograph with Otsu's thresholding.
- Fill the regions circumscribed by edges, erode the regions and then leave the largest area.
- Remove the arm region from the shortest width to the bottom of the previous binary image.
- Map to the hand radiograph and apply the line scan from top to bottom.
- Locate the local extremes of maximum. Then connect the local extremes to detect the three fingers which

were defined as the ring finger, middle finger and index finger respectively.

The physiological meanings of PROI contain three parts of joint, e.g. the EMROIs. Therefore, EMROIs can be searched out by the local extremes from the projection profile of the PROI easily (see Fig. 3a). The phalange information can be extracted from the background for identifying the three knuckles of medius and the third metacarpal. The proposed procedures are listed below:

- Rotate the finger with -90° along horizontal direction.
- Sum each column vector into a profile and then smooth the resultant profile (see Fig. 3b).
- Filter the resultant profile by using a moving average filter (see Fig. 3c).

Locate the position of the knuckle between medius and the third metacarpal by local extremes.

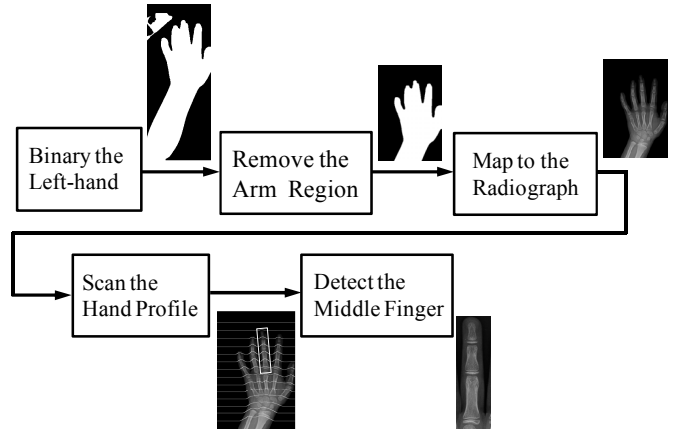


Figure 2. Schematic of detecting middle finger.

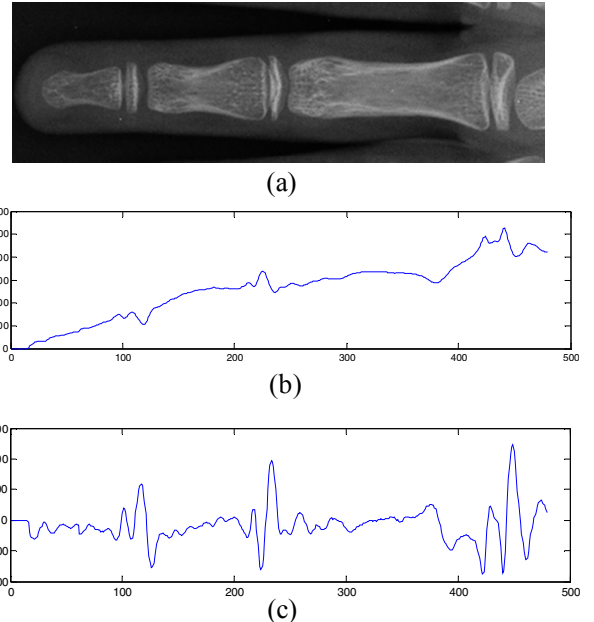


Figure 3. (a)The cropped middle finger. (b) Profile of the accumulated gray-level intensity of (a). (c) Profile of (b) subtraction by using its moving average filter.

A. Neutrosophic theory

In neutrosophic theory, each event can be seen as a certain degree of truth, falsity and indeterminacy, which are independently from each other [9]. Thus, for a theory, event, concept, or entity, $\{A\}$ is existed with its opposite $\{\text{Anti-}A\}$ and the neutrality $\{\text{Neut-}A\}$ simultaneously. On the contrary, the $\{\text{Neut-}A\}$ and $\{\text{Anti-}A\}$ are represented to as $\{\text{Non-}A\}$. According to this theory, each event $\{A\}$ is playing a role of neutralization between $\{\text{Anti-}A\}$ and $\{\text{Non-}A\}$. For example, if $\langle A \rangle = \text{white}$, then $\langle \text{Anti-}A \rangle = \text{black}$, $\langle \text{Non-}A \rangle = \text{black, gray, and intermediate states between them, and } \langle \text{Neut-}A \rangle = \text{intermediate states between them but excluding the white and black, etc. Such an idea serves a novelty to cope with the indeterminate problem, i.e. the image with uncertainty information. In this section, neutrosophic set was introduced into our study for implementing the segmentation of the EMROIs, and the descriptions were defined as below.}$

B. Neutrosophic set:

In this paper, the boundary information between the bony and soft tissue are unclear and hard to detect. Therefore, a pixel of an image, $P(i, j)$, can be used as an alternative indication of $P = \{t, i, f\}$, which represents the pixel is $t\%$ true (EMROIs), $i\%$ intermediate (bony boundaries), and $f\%$ false (others), where $t \in T$, $i \in I$ and $f \in F$, and T , I and F indicate true, indeterminacy and false domains individually [8,11]. Traditionally, fuzzy set can be regarded as $i = 0$, and $0 \leq t, f \leq 100$; however, a neutrosophic set is defined as $0 \leq t, i, f \leq 100$. Thus, we can apply the property by a three-level model to make the segmentation more adaptive.

In the computation, the pixel $P(i, j)$ in the image domain is transformed into the neutrosophic domain, $P_{NS}(i, j) = \{T(i, j), I(i, j), F(i, j)\}$, and the formulations can be defined as:

$$T(i, j) = \frac{\bar{g}(i, j) - \bar{g}_{\min}}{\bar{g}_{\max} - \bar{g}_{\min}} \quad (1)$$

$$\bar{g}(i, j) = \frac{1}{w \times w} \sum_{m=i-w/2}^{i+w/2} \sum_{n=j-w/2}^{j+w/2} g(m, n) \quad (2)$$

$$I(i, j) = \frac{\delta(i, j) - \delta_{\min}}{\delta_{\max} - \delta_{\min}} \quad (3)$$

$$\delta(i, j) = abs(g(i, j) - \bar{g}(i, j)) \quad (4)$$

$$F(i, j) = 1 - T(i, j) \quad (5)$$

where $g(i, j)$ and $\bar{g}(i, j)$ is the intensity and local mean intensity of the image at the position (i, j) .

1) α -mean operation:

The α -mean operation for P_{NS} , $P_{NS}(\alpha)$ is shown as:

$$\bar{P}_{NS}(\alpha) = P(\bar{T}(\alpha), \bar{I}(\alpha), \bar{F}(\alpha)) \quad (6)$$

where

$$\bar{T}(\alpha) = \begin{cases} T, & I < \alpha \\ \bar{T}_\alpha, & I \geq \alpha \end{cases} \quad (7)$$

$$\bar{T}_\alpha(i, j) = \frac{1}{w \times w} \sum_{m=i-w/2}^{i+w/2} \sum_{n=j-w/2}^{j+w/2} T(m, n) \quad (8)$$

$$\bar{F}(\alpha) = \begin{cases} F, & I < \alpha \\ \bar{F}_\alpha, & I \geq \alpha \end{cases} \quad (9)$$

$$\bar{F}_\alpha(i, j) = \frac{1}{w \times w} \sum_{m=i-w/2}^{i+w/2} \sum_{n=j-w/2}^{j+w/2} F(m, n) \quad (10)$$

$$\bar{I}_\alpha(i, j) = \frac{\bar{\delta}_T(i, j) - \bar{\delta}_{T_{\min}}}{\bar{\delta}_{T_{\max}} - \bar{\delta}_{T_{\min}}} \quad (11)$$

$$\bar{\delta}_T(i, j) = abs(\bar{T}(i, j) - \bar{\bar{T}}(i, j)) \quad (12)$$

$$\bar{\bar{T}}(i, j) = \frac{1}{w \times w} \sum_{m=i-w/2}^{i+w/2} \sum_{n=j-w/2}^{j+w/2} \bar{T}(m, n) \quad (13)$$

where $\bar{T}(i, j)$ and $\bar{\bar{T}}(i, j)$ are the mean intensity and the corresponding mean value after the α -mean operation. After the α -mean operation, the distribution of each element in I becomes more uniform and therefore the entropy of the indeterminacy I can be improved. In this experiment, α is selected as 0.9 by empirically experiments.

2) β -enhancement operation:

A β -enhancement operation for P_{NS} , $P_{NS}(\beta)$ is formulated as:

$$P'_{NS}(\beta) = P(\bar{T}'(\beta), \bar{I}'(\beta), \bar{F}'(\beta)) \quad (14)$$

where

$$T'(\beta) = \begin{cases} T, & I < \beta \\ T_\lambda, & I \geq \beta \end{cases} \quad (15)$$

$$T'_\beta(i, j) = \begin{cases} 2T^2(i, j), & T(i, j) \leq 0.5 \\ 1 - 2(1 - T(i, j))^2, & T(i, j) > 0.5 \end{cases} \quad (16)$$

$$F'(\beta) = \begin{cases} F, & I < \beta \\ F'_\lambda, & I \geq \beta \end{cases} \quad (17)$$

$$F'_\beta(i, j) = \begin{cases} 2F^2(i, j), & F(i, j) \leq 0.5 \\ 1 - 2(1 - F(i, j))^2, & F(i, j) > 0.5 \end{cases} \quad (18)$$

$$I'_\beta(i, j) = \frac{\delta'_T(i, j) - \delta'_{T_{\min}}}{\delta'_{T_{\max}} - \delta'_{T_{\min}}} \quad (19)$$

$$\delta_T(i, j) = abs(T'(i, j) - \bar{T}'(i, j)) \quad (20)$$

$$\bar{T}'(i, j) = \frac{1}{w \times w} \sum_{m=i-w/2}^{i+w/2} \sum_{n=j-w/2}^{j+w/2} T'(m, n) \quad (21)$$

where $T'(i, j)$ and $\bar{T}'(i, j)$ are the intensity and its local mean value after the β -enhancement operation. After the β -enhancement operation, the membership set T becomes more

distinct for the purpose of segmentation. Also, β is selected as 0.9 in our experiments.

3) Neutrosophic entropy:

The entropy of the neutrosophic image is applied to the employment of estimating the gray-level image histogram as a probability distribution, and the summed entropies of the three sets, T, I and F, are shown

$$En_{NS} = En_T + En_I + En_F \quad (22)$$

$$En_T = - \sum_{i=\min\{T\}}^{\max\{T\}} p_T(i) \ln p_T(i) \quad (23)$$

$$En_I = - \sum_{i=\min\{I\}}^{\max\{I\}} p_I(i) \ln p_I(i) \quad (24)$$

$$En_F = - \sum_{i=\min\{F\}}^{\max\{F\}} p_F(i) \ln p_F(i) \quad (25)$$

where En_T , En_I and En_F are the entropies of the sets T, I, and F individually, whose values equal to the element i in T , I and F .

4) K-means clustering analysis on neutrosophic set

Because clustering method can effectively categorize similar pixels into the same group [11], the $P_{NS}(\alpha, \beta)$ which was proceed by the α -mean operation and β -enhancement operation can be applied to classification. To consider $\bar{T}'(i, j)$ as an unclassified data set, the clustering problem means to classify the $\bar{T}'(i, j)$ into m partitions which were represented as $C = \{C_j, j=1,2,\dots,m\}$. Here, the employed K-means algorithm as the clustering method, is defined as

$$J_c = - \sum_{j=1}^m \|T(i, j) - Z_j\| \quad (26)$$

where Z_j is the centroid of the j th cluster and m is the amount of clusters. Additionally, the necessary definition of the minimum J_c is

$$Z_j = \frac{1}{n_j} \sum_{X_i \in C_j} X_i \quad (27)$$

where n_j is the number of pixels in the j th cluster, C_j .

C. Apply the NS algorithm to EMROI

The related algorithm is summarized in the following steps:

- Input the image and transfrom the image into NS domain by Eqs. (1)-(5);
- Perform the α -mean operation and β -enhancement operation on the subset T by Eqs. (6)-(21);
- Compute the entropy of the indeterminate subset I, $En_I(i)$ by Eqs. (22)-(25);
- If $(En_I(i+1) - En_I(i))/En_I(i)$ less than δ , apply the K-means clustering algorithm to the subset T; else go to Step (b).

- Finally, we can obtain the EMROI segmentation.

III. RESULTS AND DISCUSSION

The procedures based on NS for EMROI segmentation was demonstrated in Figure 4. In this framework, the EMROI was operated by using the NS operation as the first step, to let the bony tissue more distinct. Subsequently, the enhanced EMROI was categorized by K-means method as white color, gray color and black color, in the second step. The region with highest centroid, i.e. with white color, was chosen as the EMROI in the third step. In the fourth step, due to some broken holes in EMROI, the process of performing a flood-fill operation is employed, and the segmented EMROI was completed. Because the bony and soft tissue contains nonuniform gray-levels, it can be concluded that the higher gray-levels indicates the mixture of bony and soft tissue, and the lower gray-levels corresponds to the soft tissue and background. The image segmentation scheme serves robustness against these poor images.

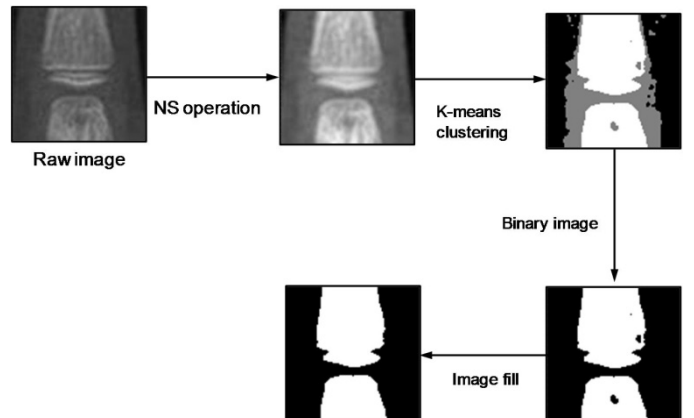


Figure 4. The procedures of performing EMROIs segmentation.

Here, the segmentation performances based on the NS enhancement for three ages of 3 years, 8 years and 12 years individually, are given in Figure 5-7. Figure 5(a)-(c) are displayed the original EMROIs with the distal, middle, and proximal and their corresponding segmentation results are shown in Figure (d)-(f). Another two examples are also demonstrated in Figure 6 and 7. Evidently, our proposed segmentation scheme is very close to the observation; despite a little defect occurred, e.g. the Figure 5(e), (f) and Figure 6 (f), the most important regions of EMROIs and the corresponding physiological features are still preserved.

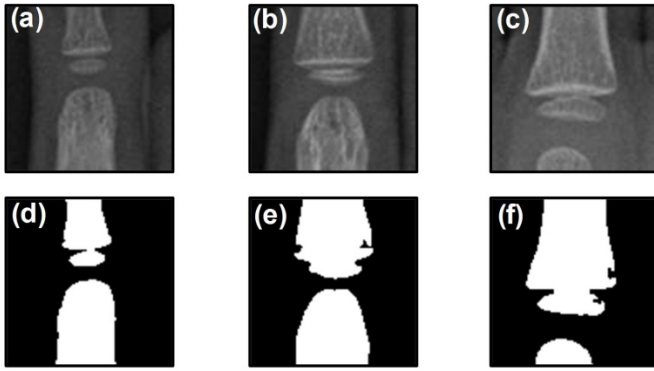


Figure 5. A 3 years girl with three cropped EMROIs and their corresponding segmented results.

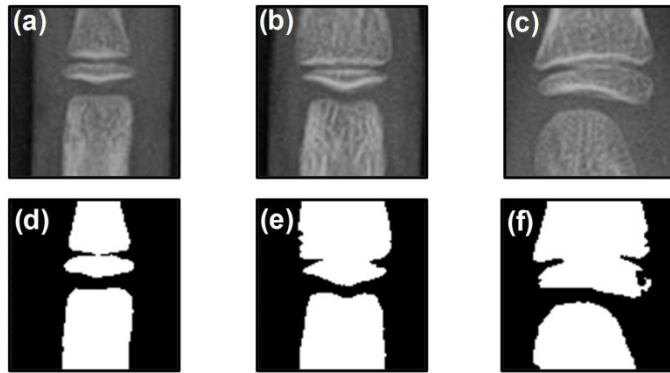


Figure 6. A 8 years girl with three cropped EMROIs and their corresponding segmented results.

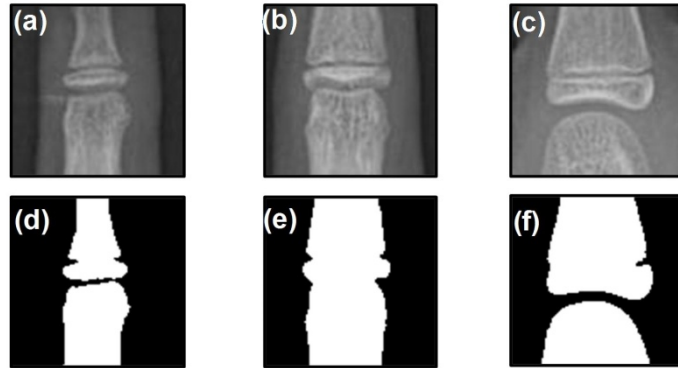


Figure 7. A 12 years girl with three cropped EMROIs and their corresponding segmented results.

IV. CONCLUSIONS

In this study, a novelty of NS approach to EMROIs segmentation is introduced. Based on the α -mean operation and β -enhancement operation, the structure of the image becomes uniform but with distinct edges. Finally, the segmentation algorithm based on the k-means clustering method was proposed to segment the EMROIs from the background and soft tissue. The demonstrated results reveal that the method can help to segment the bony tissue precisely for assisting the BAA and monitoring the growth therapies.

REFERENCES

- [1] W. W. Greulich, S. I. Pyle, and T. W. Todd, *Radiographic atlas of skeletal development of the hand and wrist*. Stanford University Press, Stanford, 1950.
- [2] T. W. Todd, *Atlas of skeletal maturation*, Mosby, St. Louis, 1937.
- [3] A. Zhang, A. Gertych, B. J. Liu, "Automatic bone age assessment for young children from newborn to 7-year-old using carpal bones," *Comput. Med. Imag. Grap.*, vol.31(4-5), pp.299–310, 2007.
- [4] E. Pietka, A. Gertych, S. Pośpiech, F. Cao, H. K. Huang and V. Gilsanz, "Computer-assisted bone age assessment: image preprocessing and epiphyseal/metaphyseal ROI extraction," *IEEE Trans. Med. Imag.*, vol. 20(8), pp.715–729, 2001.
- [5] C. W. Hsieh, T. C. Liu, T. L. Jong, C. M. Tiu, "A fuzzy-based growth model with principle component analysis selection for carpal bone-age assessment. *Med. Biol. Eng. Comput.*, vol.48(6), pp.579–588, 2010.
- [6] C. W. Hsieh, T. C. Liu, T. L. Jong, C. Y. Chen, C. M. Tiu, and D. Y. Chan, "Fast and fully automatic phalanx segmentation using a grayscale-histogram morphology algorithm," *Opt. Eng.*, vol.50(8), pp.087007–087007-14, 2011.
- [7] C. W. Hsieh, C. Y. Chen, T. L. Jong, T. C. Liu, C. H. Chiu, "Automatic Segmentation of Phalanx and Epiphyseal/Metaphyseal Region by Gamma Parameter Enhancement Algorithm," *Meas Sci. Rev.*, vol.12(1), pp. 21–27, 2012.
- [8] Y. Guo and H. D. Cheng, "A new neutrosophic approach to image segmentation", *Pattern Recogn.*, vol.42, pp.587–595, 2009.
- [9] F. Smarandache, *A Unifying Field in Logics Neutrosophic Logic. Neutrosophy, Neutrosophic Set, Neutrosophic Probability*, third ed., American Research Press, 2003.
- [10] B. E. Pietka , S. Pośpiech , A. Gertych , F. Cao , H.K. Huang and V. Gilsanz. "Computer automated approach to the extraction of epiphyseal regions in hand radiographs", *J. Digit. Imaging*, vol.14(4), pp.165–172.
- [11] R. O. Duda, P. E. Hart and D. G. Stork, *Pattern Classification*, Wiley-Interscience, New York, 2000.